Interactions between Bacteriophage DNA and Cationic Biomimetic Particles

ARTICLE *in* THE JOURNAL OF PHYSICAL CHEMISTRY B · JANUARY 2009

Impact Factor: 3.3 · DOI: 10.1021/jp806992f · Source: PubMed

3 AUTHORS, INCLUDING:

Heloísa Rosa
Universidade Federal de São Paulo
4 PUBLICATIONS **37** CITATIONS
SEE PROFILE

Ana M Carmona-Ribeiro
University of São Paulo
137 PUBLICATIONS **2,541** CITATIONS
SEE PROFILE

Interactions between Bacteriophage DNA and Cationic Biomimetic Particles

Heloísa Rosa,[†] Denise F. S. Petri,[‡] and Ana M. Carmona-Ribeiro*,[†]

Departamento de Bioquímica, Departamento de Química Fundamental, Instituto de Química, Universidade de São Paulo, P.O. Box 26077, São Paulo, SP, 05513-970, Brazil

Received: August 5, 2008; Revised Manuscript Received: October 14, 2008

The interaction between giant bacteriophage DNA and cationic biomimetic particles was characterized from sizing by dynamic light-scattering, ζ-potential analysis, turbidimetry, determination of colloid stability, visualization from atomic force microscopy (AFM), and determination of cytotoxicity against *E. coli* from colony forming unities counting. First, polystyrene sulfate (PSS) particles with different sizes were covered by a dioctadecyldimethylammonium bromide (DODAB) bilayer yielding the so-called cationic biomimetic particles (PSS/DODAB). These cationic particles are highly organized, present a narrow size distribution and were obtained over a range of particle sizes. Thereafter, upon adding λ, T5 or T2-DNA to PSS/DODAB particles, supramolecular assemblies PSS/DODAB/DNA were obtained and characterized over a range of DNA concentrations and particle sizes (80−700 nm). Over the low DNA concentration range, PSS/DODAB/DNA assemblies were cationic, colloidally stable with moderate polydispersity and highly cytotoxic against *E. coli*. From DNA concentration corresponding to charge neutralization, neutral or anionic supramolecular assemblies PSS/DODAB/DNA exhibited low colloid stability, high polydispersity and moderate cytotoxicity. Some nucleosome mimetic assemblies were observed by AFM at charge neutralization (ζ-potential equal to zero).

Introduction

A variety of cationic agents have been employed for DNA compaction such as cationic peptides and proteins,[1] cationic lipids,[2] cationic polyelectrolytes, cationic surfactants, or iron(III).[3] DNA compaction has also been used to model chromatin structure and its influence on gene expression. The fundamental particle of chromatin structure is a self-assembled complex of basic histone proteins wrapped by approximately two turns of DNA.[4] This unit called "nucleosome" is the building block in a structure that compacts DNA of lengths on the order of meters into an ∼10 μm diameter cell nucleous. Phage DNA has long attracted interest on account of its seeming tractability. Phage DNA is remarkable for its density of packing, both relative and absolute. For example, in solution the 40 kbp T7 genome with its contour length of 13.6 μm might span a space several micrometers across and in an infected bacterium, ∼1 μm across. Thus, confinement to a 55 nm capsid represents a compaction marked by a density increase by a factor of $\sim 10^4$.[5] Zinchenko et al. (2007)[6] previously studied the physical chemistry of the association between cationic nanoparticles and DNA, mapping out rather complex phase diagrams as a function of particle size and concentration.[7] The way in which positively charged nanoparticles tie up DNA is not obvious, and mechanisms change dramatically with particle size.[8] Only the smallest (10 nm) particles allowed transcription to occur at intermediate loading densities. Larger particles shut transcription down rather abruptly.[6]

Cationic nanoparticles have found many uses such as efficient cell transfection agents in vitro,[9−11] visualization, and quantification of biopolymer molecules immobilized on solid support[12] and complexation with long-chained DNA as a simple model of chromatin for transcription studies.[6,13] The compaction of long duplex DNA by cationic nanoparticles (NP) used as a primary model of histone core particles has been systematically studied by Zinchenko et al. (2007) regarding the effect of salt concentration, particle size, and particle charge by means of single-molecule observations from fluorescence and transmission electron microscopy.[13] They found that DNA compaction proceeds through the formation of beads-on-a-string structures of various morphologies with DNA adsorbed amount per particle depending weakly on NP concentration but increasing with particle size and being optimal at an intermediate salt concentration.[13] Three different complexation mechanisms were proposed: free DNA adsorption onto NP surface, DNA wrapping around NP, and NP collection on DNA chain.[13]

On the other hand, particle size has been recognized as an important parameter that determines the mechanism of particle entry into cells. Particles with a diameter of 200 nm or less enter cells almost exclusively via the clathrin-coated pathway whereas particles with a larger diameter penetrate cells via caveolae-mediated endocytosis.[14,15]

Cationic biomimetic particles produced from adsorption of dioctadecyldimethylammonium bromide (DODAB) bilayers onto polystyrene sulfate (PSS) microspheres have been described by our group since 1992.[16−21] These cationic bilayer-covered particles exhibit a narrow size distribution and can be produced at any desired size ranging from 70−500 nm of mean hydrodynamic diameter.[17] In this work, they were obtained over a range of particle sizes in order to study their interaction with three different bacteriophage DNAs from a systematic dynamic light scattering study. Supramolecular assemblies were characterized from sizing, ζ-potential analysis, polydispersity, determination of colloid stability, and visualization by means of atomic force microscopy (AFM). The low colloid stability observed for the supramolecular assemblies could be associated

* To whom correspondence should be addressed. E-mail: amcr@usp.br. Phone: 0055 11 3091 3810 ext 237. Fax: 0055 11 3818 5579.
[†] Departamento de Bioquímica.
[‡] Departamento de Química Fundamental.

10.1021/jp806992f CCC: $40.75
Published on Web 12/02/2008

TABLE 1: Physical Properties of Polystyrene Sulfate (PSS) Particles As Provided by the Supplier

latex	mean diameter (nm)	surface charge density (μC/cm^2)	area per charge group (nm^2)	specific surface area (cm^{2}g^{-1})	particles concentration (particles/mL)
PSS83	83 ± 5%	1.84	8.7	685 205	2.69×10^{14}
PSS137	137 ± 2%	0.79	20.1	415 124	5.97×10^{13}
PSS301	301 ± 2%	1.68	9.5	188 944	5.87×10^{12}
PSS526	526 ± 5%	4.95	3.3	108 122	1.34×10^{12}
PSS626	626 ± 2%	6.43	2.5	90 850	7.44×10^{11}

TABLE 2: Physical Properties of λ, T5, and T2 Bacteriophages DNA

DNA type	molecular weight (Da)	DNA size (bp)
λ	31.5×10^6	48 502
T5	68×10^6	103 000
T2	110×10^6	164 000

with formation of nucleosome-mimetic systems that visibly flocculated over a range of DNA concentrations.

Material and Methods

Dioctadecyldimethylammonium bromide (DODAB) 99.9% pure was obtained from Sigma-Aldrich (St Louis, MO). Anionic polystyrene sulfate (PSS) particles, nominal mean diameters of 85 ± 5, 137 ± 2, 301 ± 2, 526 ± 5, and 626 ± 2% (Lot 10-277-71, 10-307-57, 10-66-58, 10-182-13, and 10-185-22, respectively) were purchased from Interfacial Dynamics Corporations (Portland, OR) (see Table 1) and stock suspensions containing 2.6×10^{11}, 9.6×10^{10}, 2×10^{10}, 6.6×10^9, and 4.6×10^9 particles/mL, respectively, were prepared in 1 mM NaCl, which is an adequate ionic strengh to assemble DODAB BF as a single bilayer onto particles.[19] In Table 1, particle size was determined from transmission electron microscopy and surface charge density was determined from conductometric titration by the supplier. The nanoparticles are similar to those used in our previous study.[17] DNA from phages λ (λ-DNA), T5 (T5-DNA), and T2 (T2-DNA) were purchased from Sigma at initial concentrations of 565, 505, and 128.5 μg/mL, respectively, and diluted to the desired final concentrations over a range of 1 at 10 μg/mL DNA. Details on physical properties of λ, T5, and T2-DNA taken from textbooks are given in Table 2. Milli-Q water was used to prepare all solutions and dispersions throughout.

Preparation of DODAB Dispersions. Small DODAB bilayer fragments (BF), 65 ± 2 nm mean diameter and 45 ± 2 mV mean ζ-potential, were prepared by sonication with titanium macrotip probe in 1 mM NaCl water solution at ca. 2.0 mM DODAB as previously described.[22] Analytical concentrations of DODAB or NaCl were determined by halide microtitration.[23]

Preparation of PSS/DODAB and PSS/DODAB/DNA Assemblies. For dispersions of PSS301 as an example, particles at 2×10^{10} particles/mL and stock DODAB bilayer fragments BF dispersions at 2.0 mM DODAB, both in 1 mM NaCl were diluted to the final desired concentration using this same salt solution. Thus, 0.5 mL of the stock PSS dispersion, 0.02 mL of a 2 mM DODAB BF dispersion, and 1.480 mL of a 1 mM NaCl solution were mixed and allowed to interact for 1 h at 25 °C yielding 5×10^9 PSS particles/mL and 0.02 mM DODAB. This last concentration is the one slightly above the one required to cover each particle with a DODAB bilayer.[16,24] Considering the total PSS area of 1.43×10^{-3} m^2, a DODAB concentration of 0.007 mM would be precisely sufficient to produce bilayer-covered particles so that DODAB BF would not be expected to be found free in dispersion.[16,24,25] For the other particulates, PSS particles (2.6×10^{11}, 9.6×10^{10}, 2×10^{10}, 6.6×10^9, and 4.6×10^9/mL) and DODAB lipid BF (2.0 mM) were always prepared in 1 mM NaCl and diluted to the final desired concentration using this same salt solution. PSS microspheres with surface area equal to 1.43×10^{-3} m^2 at final concentrations of 6.6×10^{10}, 2.4×10^{10}, 5×10^9, 1.6×10^9, 1.2×10^{10} particles/mL and DODAB dispersions (1×10^{-4} to 5×10^{-2} mM) interacted for 1 h/25 °C. DODAB final concentration for producing the assemblies was selected as 0.02 mM at 6.6×10^{10}, 2.4×10^{10}, 5×10^9, 1.6×10^9, 1.2×10^{10} particles per milliliter since this concentration is slightly above the one required to cover each nanosphere with a DODAB bilayer. Positively charged and stable particles upon deposition of one bilayer were obtained from 10^{-3} mM DODAB (Table 3). In a second experimental step, DNA was added to the PSS/DODAB mixtures at final concentrations ranging from 1 to 10 μg/mL for λ, T5, and T2-DNA for 1 h/25 °C. Thereafter, sizes, ζ-potentials, and polydispersities were determined. Details on particle number densities, DODAB concentrations and/or DNA concentrations are given on Tables 4 and 5.

Determination of Size, Size Distribution, Polydispersity, and ζ-potentials for DODAB BF, PSS, PSS/DODAB, and PSS/DODAB/DNA Dispersions. Particle size (mean diameter D_z), size distribution, polydispersity and ζ-potential in the presence or absence of PSS, DODAB, or DNA were determined using the ZetaPlus-ZetaPotential Analyzer (Brookhaven Instruments Corporation, Holtsville, NY), which was equipped with a 677 nm laser and dynamic light-scattering (PCS) at 90° for particle sizing. From fluctuations of scattered light intensity, the decay times of the fluctuations can be related to the diffusion constants and, therefore, to the sizes of the particles. Small particles moving rapidly cause faster decaying fluctuations than large particles moving slowly. The decay times of theses fluctuations is determined in the time domain using a correlator. The fluctuating signal is processed by forming the autocorrelation function which decays exponentially with time so that the relaxation of the fluctuations is directly related to the decay constant (Γ). The decay constant is given by:

$$\Phi = Dq^2 \tag{1}$$

where q depends on the scattering angle, the wavelenght of the laser light and refractive index of the suspending liquid and D is the translational diffusion coefficient. Hydrodynamic particle diameter (D_z) is inversely related to D by the Stokes−Einstein equation

$$D_z = kT/(3\pi\eta D) \tag{2}$$

where k is the Boltzmann's constant, T is temperature in Kelvin, η is the viscosity of the suspending liquid, and D is the diffusion coefficient. Mean diameters were obtained by fitting data to log-normal size distributions that does not discriminate between one, two, or more different populations and considers always all scattering particles as belonging to one single Gaussian population. For the size distribution data, fitting was performed by the apparatus

TABLE 3: DODAB Concentrations Required for Charge Neutralization of PSS Particles or for Preparation of the Cationic Biomimetic Particles[a]

latex	particles concentration (particles/mL)	[DODAB] for zero ζ-potential/mM	[DODAB] for maximal aggregation/mM	[DODAB] for minimal size and positive ζ-potential/mM
PSS83	6.6×10^{10}	8×10^{-4}	6×10^{-4}	5×10^{-3}
PSS137	2.4×10^{10}	8×10^{-4}	6×10^{-4}	5×10^{-3}
PSS301	5.0×10^{9}	6×10^{-4}	6×10^{-4}	5×10^{-3}
PSS526	1.6×10^{9}	2×10^{-3}	1×10^{-3}	10×10^{-3}
PSS626	1.2×10^{9}	2×10^{-3}	1×10^{-3}	10×10^{-3}

[a] The theoretical DODAB concentration value for covering all PSS particles with one DODAB bilayer is 7×10^{-3} mM when total surface area for each particulate is 1.43×10^{-3} m^2.

TABLE 4: Mean Sizes, ζ-Potentials, and Polydispersities for PSS137 at 2.4×10^{10} particles/mL, DODAB Dispersion and PSS/DODAB/DNA Supramolecular Assemblies over a Range of [DNA] at [DODAB] = 0.02 mM

assemblies	[DNA] (μg/mL)	mean diameter (nm)	ζ-potential (mV)	Polydispersity
PSS137		133 ± 1	−35 ± 2	0.059 ± 0.007
DODAB (2 mM)		65 ± 2	45 ± 2	0.289 ± 0.006
PSS137/DODAB		149 ± 1	30 ± 2	0.049 ± 0.014
PSS137/DODAB/λ-DNA	1	169 ± 1	21 ± 2	0.096 ± 0.012
	2	230 ± 1	22 ± 2	0.152 ± 0.017
	3	223 ± 2	19 ± 2	0.158 ± 0.019
	4	267 ± 2	17 ± 2	0.163 ± 0.013
	5	3316 ± 175	2 ± 1	0.278 ± 0.053
	6	2687 ± 223	2 ± 1	0.387 ± 0.033
	7	244 ± 2	−26 ± 2	0.122 ± 0.017
	8	213 ± 1	−27 ± 2	0.177 ± 0.013
	9	234 ± 1	−21 ± 2	0.167 ± 0.015
	10	198 ± 3	−22 ± 2	0.183 ± 0.010
PSS137/DODAB/T5-DNA	1	200 ± 2	22 ± 2	0.136 ± 0.038
	2	258 ± 2	32 ± 2	0.236 ± 0.013
	3	457 ± 4	28 ± 2	0.281 ± 0.008
	4	404 ± 4	21 ± 2	0.285 ± 0.008
	5	384 ± 6	16 ± 2	0.247 ± 0.009
	6	467 ± 6	15 ± 4	0.282 ± 0.013
	7	2214 ± 67	2 ± 3	0.368 ± 0.032
	8	333 ± 3	−24 ± 2	0.229 ± 0.012
	9	313 ± 6	−31 ± 4	0.273 ± 0.017
	10	309 ± 3	−45 ± 3	0.243 ± 0.009
PSS137/DODAB/T2-DNA	1	174 ± 2	17 ± 1	0.122 ± 0.022
	2	269 ± 7	22 ± 2	0.293 ± 0.015
	3	329 ± 2	11 ± 1	0.245 ± 0.013
	4	340 ± 7	10 ± 2	0.232 ± 0.006
	5	1081 ± 94	8 ± 2	0.370 ± 0.006
	6	1644 ± 120	−1 ± 2	0.342 ± 0.025
	7	4918 ± 3348	4 ± 2	0.321 ± 0.050
	8	16669 ± 5372	−30 ± 4	0.446 ± 0.062
	9	2407 ± 1229	−46 ± 2	0.367 ± 0.024
	10	1874 ± 721	−49 ± 3	0.346 ± 0.045

software using the non-negatively constrained least-squares (NNLS) algorithm, which is a model independent technique allowing to achieve multimodal distributions.[26] In order to define a relative width of size distributions, the polydispersity or polydispersity index is given by

$$\text{Polydispersity} = \mu_2/\Gamma^2 \quad (3)$$

where μ_2 is proportional to the variance of the "intensity" weighted diffusion coefficient distribution and carries information on the width of the size distribution. Polydispersity has no units. It is close to zero (0.000 to 0.020) for monodisperse or nearly monodisperse samples, small (0.020 to 0.080) for narrow distributions, and larger for broader distributions. ζ was determined from eletrophoretic mobility μ in 1 mM NaCl and the Smoluchowski's equation

$$\zeta = \mu\eta/\varepsilon \quad (4)$$

where η is the medium viscosity and ε the medium dieletric constant.

Determination of Turbidity Kinetics, Dispersions Photographs, AFM Topographic Images, and Colloid Stability for PSS/DODAB/DNA Assemblies. The turbidity kinetics of PSS301/DODAB/DNA assemblies was determined from turbidity measurements at 400 nm using a UV−vis spectrophotometer Hitachi 2000 during 30 min in glass cuvettes. Macroscopic visualization of PSS137/DODAB/T2-DNA or PSS301/DODAB/T2-DNA assemblies dispersed in 1 mM NaCl water solutions were obtained using a digital camera Sony/Cyber-shot 3.2 megapixels over a range of T2-DNA concentrations. The final concentrations of PSS137, PSS301, and DODAB were 2.4×10^{10} particles/mL, 5×10^{9} particles/mL, and 0.02 mM, respectively. AFM topographic images for the PSS137/DODAB/T2-DNA dispersion were obtained by means of a PicoSPM-LE molecular imaging system with cantilevers operating in the intermittent-contact mode (AAC mode) at a resonance frequence of approximately 302 kHz. All topographic images represent original data and refer to scan area of (10×10) μm^2 with a resolution of (512×512) pixels.

TABLE 5: Mean Sizes, ζ-Potentials, and Polydispersities for PSS301 at 5×10^9 particles/mL, DODAB Dispersion, and PSS/DODAB/DNA Supramolecular Assemblies over a Range of [DNA] at [DODAB] = 0.02 mM

assemblies	[DNA] (μg/mL)	mean diameter (nm)	ζ-potential (mV)	polydispersity
PSS301		308 ± 2	−44 ± 3	0.038 ± 0.005
DODAB (2 mM)		65 ± 2	45 ± 2	0.289 ± 0.006
PSS301/DODAB		309 ± 3	54 ± 2	0.030 ± 0.021
PSS301/DODAB/λ-DNA	1	351 ± 4	53 ± 1	0.128 ± 0.028
	2	412 ± 3	39 ± 1	0.159 ± 0.026
	3	404 ± 4	25 ± 3	0.145 ± 0.039
	4	1363 ± 34	22 ± 1	0.310 ± 0.006
	5	2741 ± 287	11 ± 1	0.336 ± 0.014
	6	2039 ± 49	−5 ± 2	0.365 ± 0.028
	7	2011 ± 79	7 ± 1	0.245 ± 0.036
	8	502 ± 3	−37 ± 2	0.192 ± 0.017
	9	456 ± 3	−38 ± 2	0.192 ± 0.021
	10	439 ± 2	−42 ± 2	0.195 ± 0.015
PSS301/DODAB/T5-DNA	1	333 ± 4	45 ± 3	0.130 ± 0.028
	2	351 ± 4	40 ± 1	0.105 ± 0.034
	3	412 ± 5	39 ± 3	0.147 ± 0.027
	4	528 ± 10	30 ± 1	0.240 ± 0.016
	5	2403 ± 72	8 ± 1	0.315 ± 0.023
	6	2553 ± 72	6 ± 1	0.318 ± 0.027
	7	549 ± 7	−25 ± 2	0.236 ± 0.016
	8	480 ± 5	−36 ± 2	0.245 ± 0.013
	9	547 ± 6	−50 ± 2	0.244 ± 0.016
	10	476 ± 4	−50 ± 3	0.212 ± 0.010
PSS301/DODAB/T2-DNA	1	430 ± 3	33 ± 3	0.252 ± 0.014
	2	615 ± 4	23 ± 2	0.280 ± 0.011
	3	623 ± 6	19 ± 2	0.286 ± 0.014
	4	764 ± 25	14 ± 4	0.303 ± 0.030
	5	1083 ± 29	12 ± 1	0.331 ± 0.012
	6	2240 ± 134	−5 ± 1	0.360 ± 0.025
	7	1004 ± 59	−29 ± 2	0.331 ± 0.013
	8	659 ± 39	−42 ± 2	0.287 ± 0.014
	9	637 ± 9	−52 ± 1	0.265 ± 0.017
	10	667 ± 18	−58 ± 1	0.309 ± 0.015

Organism, Culture Conditions, and Bacteria Viability Assay. *Escherichia coli (E. coli)* ATCC 25522 was reactivated for 2−5 h at 37 °C in 3 mL of tryptic soy broth, TSB (Merck KGaA, Darmstadt, Germany). Thereafter, bacteria were spread on plates of MacConkey agar (Merck KGaA, Darmstadt, Germany) and incubated (37 °C/6 h). Several colonies were then taken from plates and incubated in 50 mL of liquid TSB (160 rpm, 37 °C, 2.5 h). The culture was pelleted and separated from its nutritive medium by centrifugation (3000 rpm/5 min). The supernatant was replaced by sterile water and bacteria pellet was resuspended. The centrifugation/resuspension procedure was repeated three times before using the bacteria for evaluating viability cell from PSS/DODAB/DNA assemblies. After washing, the final pellet was resuspended in a sterile water volume sufficient to yield 0.127 absorbance unities at 600 nm, which is equivalent to 2×10^7 CFU/mL after plating. 0.5 mL of the final cell suspension was added on 0.5 mL of PSS137/DODAB/DNA or PSS301/DODAB/DNA dispersions previously prepared as described to yield concentrations quoted in each viability curve. After 1 h interactions, mixtures were diluted (1:1000) and 0.1 mL of the diluted mixtures was spread on agar plates. After spreading, plates were incubated for 24 h at 37 °C. CFU counts were obtained using a colony counter. Cell viability (%) was plotted as a function of bacteriophage DNA concentration for the three DNA tested.

Results and Discussion

Cationic Biomimetic Particles Produced over a Range of Latex Particle Size. From equivalence of total surface areas for particles and DODAB bilayers, stable, positively charged, and bilayer-covered particles can be obtained. PSS/DODAB assemblies were characterized at 1 mM NaCl over a range of PSS particles size corresponding to 6.6×10^{10}, 2.4×10^{10}, 5×10^9, 1.6×10^9, 1.2×10^{10} particles/mL over a range of increasing DODAB concentrations (1×10^{-4} to 5×10^{-2} mM) by means of dynamic light scattering for particle sizing and ζ-potential analysis. Figure 1 shows one of these DODAB concentration effects on ζ-average diameter (A) or ζ-potentials (B) for PSS particles with diameter of 301 nm at 5×10^9 PSS particles/mL. 0.02 mM DODAB produced perfectly homodisperse and cationic bilayer-covered particles. Oppositely charged biomolecules can therefore be driven to biomimetic particles via electrostatic attraction. Scheme 1 shows the general design and steps performed to obtain the interaction between bacteriophage DNA and cationic PSS/DODAB particles. In the first step, at 1 mM NaCl, the PSS polymeric particles were covered by oppositely charged DODAB bilayer fragments (BF). This procedure was previously shown to result in one bilayer coverage surrounding each particle from determination of adsorption isotherm,[22] electron transmission microscopy of positively stained bilayer-covered particles,[20] increase in the mean particle diameter of 8−10 nm as expected for deposition of one-bilayer thickness, reversal of particle ζ-potential from negative to positive and improved colloid stability at and above bilayer coverage.[18,19,22,25] Apparently, 1 mM ionic strength provided by 1 mM NaCl was effective in inducing a hydrophobically driven autoassociative process of adjacent bilayer fragments deposited onto the polymeric particles that did not take place in water or ionic strengths smaller than 1 mM.[19] At charge neutralization, there is maximal interparticle aggregation and minimal colloid stability. Further increasing DODAB

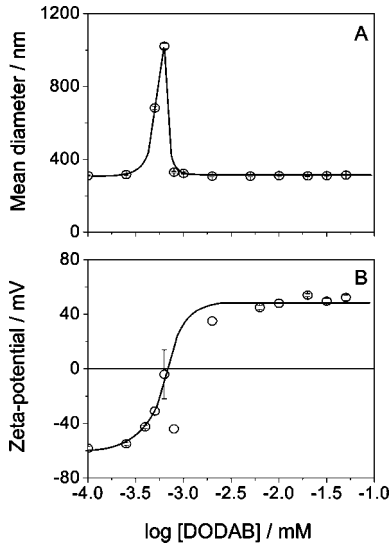

Figure 1. DODAB concentration effect on properties of PSS301 particles: ζ-average diameter (A) and ζ-potentials (B). PSS301 microspheres with surface area equal to 1.43×10^{-3} m^2 at 5×10^9 particles/mL interacted with DODAB BF over a range of DODAB concentrations (1 h/25 °C) in 1 mM NaCl water solutions before measurements.

SCHEME 1: Schematic Representation of PSS/DODAB/DNA Assemblies from Cationic Bilayer-Covered PSS and Bacteriophage DNA (in red)[a]

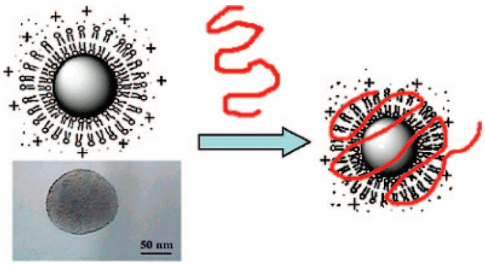

[a] A polystyrene sulfate (PSS) microsphere covered by a cationic DODAB bilayer is seen by transmission electron microscopy (TEM) thanks to ammonium molybdate positive staining of the DODAB bilayer.[18]

concentration stabilizes the system at sizes and ζ-potentials consistent with DODAB bilayer adsorption. Table 3 shows particles concentration for PSS, DODAB concentrations for zero ζ-potential, DODAB concentration for maximal aggregation and DODAB concentration for minimal size, and positive ζ over a range of high colloid stability.

The DODAB amount used to cover all particles with one cationic bilayer was slightly above the one required for bilayer deposition: 0.02 mM DODAB was more than enough to cover the whole surface area of 1.43×10^{-3} m^2 on particles with one bilayer. Figure 2 shows size distribution of PSS particles with 83 (A), 137 (B), 301 (C), 526 (D), and 626 (E) nm mean diameters at 6.6×10^{10}, 2.4×10^{10}, 5×10^9, 1.6×10^9, and 1.2×10^9 particles/mL, respectively. A remarkably narrow particle size distribution for the PSS/DODAB assemblies was obtained. In addition, PSS particles diameter increase to 108, 149, 309, 542, and 696 nm, respectively.

It is possible to calculate the number of DODAB molecules required to cover all particles with one bilayer. Assuming the area per DODAB molecule at the air−water interface equal to 0.6 nm^2,[27] 1.18×10^{15} DODAB molecules or 10^{-3} mM DODAB final concentration would be needed theoretically to bilayer-cover PSS particles in these final concentrations. Positively

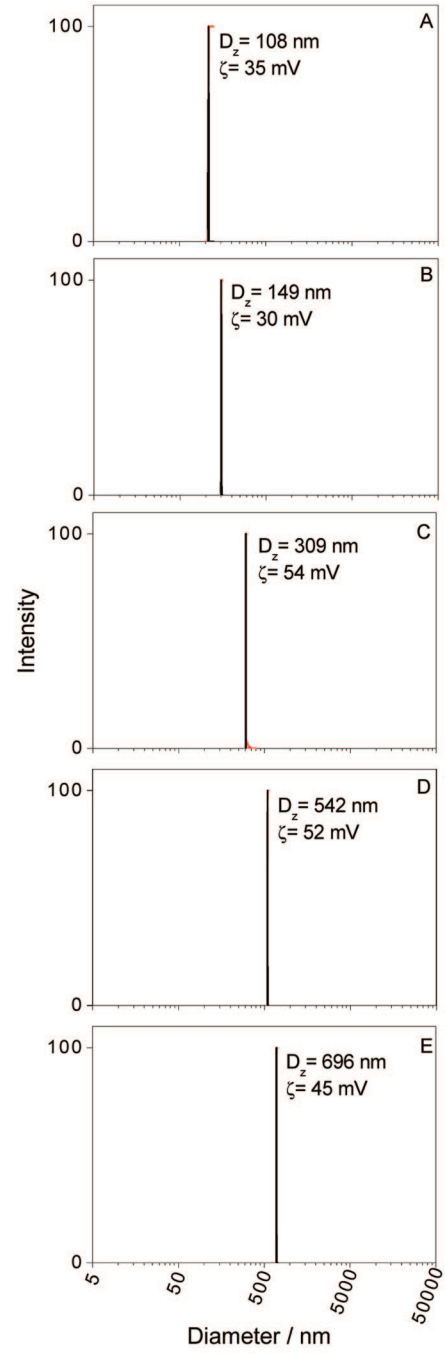

Figure 2. Size distribution of PSS/DODAB particles from 83 (A), 137 (B), 301 (C), 526 (D), and 626 nm mean diameter PSS (E) at 6.6×10^{10}, 2.4×10^{10}, 5×10^9, 1.6×10^9, and 1.2×10^9 particles/mL, respectively, and after interacting with 0.02 mM DODAB. This last [DODAB] was enough to cover 1.43×10^{-3} m^2 of total surface area on particles with one bilayer.

charged and stable particles with sizes increased by deposition of one bilayer were indeed obtained experimentally from 10^{-3} mM DODAB (Table 3). This is consistent with the ζ-potential data showing reversal of particle surface charge. Overall, the ζ-potentials for PSS/DODAB particles over a range of particle sizes were very similar to ζ-potentials for the DODAB bilayer in form of bilayer fragments (Figure 2). Table 3 shows also the DODAB concentration required for attaining minimal size. This was selected among all positively charged, bilayer-covered particles determined from the dependence of sizes and ζ-potentials on DODAB concentration (shown only for PSS301 particles).

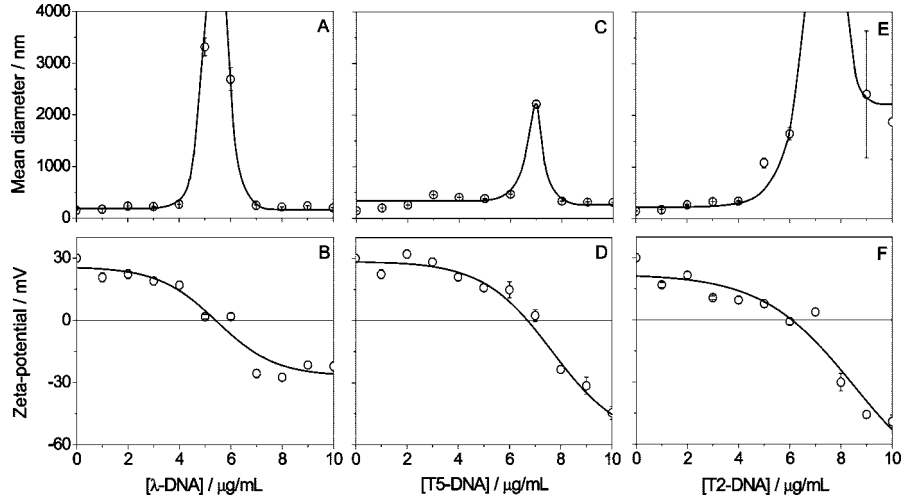

Figure 3. Effect of λ-, T5-, and T2-DNA concentration on ζ-average diameter (A,C,E) and ζ-potentials (B,D,F) of PSS137/DODAB nanoparticles. PSS137 microspheres with surface area equal to 1.43×10^{-3} m^2 and final concentrations of 2.4×10^{10} particles/mL interacted (1 h/25 °C) with 0.02 mM DODAB BF in order to obtain cationic, bilayer-covered biomimetic particles. Thereafter, DNA over a range of concentrations was added for interaction with biomimetic PSS/DODAB particles (1 h/25 °C).

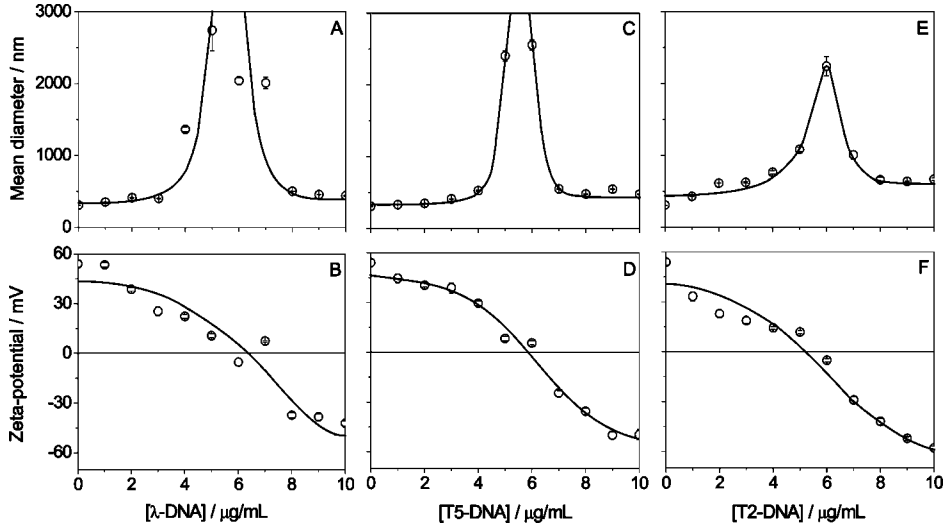

Figure 4. Effect of λ, T5, and T2-DNA concentration on ζ-average diameter (A,C,E) and ζ-potentials (B,D,F) of PSS301/DODAB nanoparticles. PSS301 microspheres with surface area equal to 1.43×10^{-3} m^2 and final concentrations of 5×10^9 particles/mL interacted (1 h/25 °C) with 0.02 mM DODAB BF in order to obtain cationic biomimetic particles. Thereafter, DNA over a range of concentrations was added for interaction with biomimetic PSS/DODAB particles (1 h/25 °C).

Interaction of Cationic Biomimetic Particles of Different Sizes with Three Different Bacteriophage DNAs. Polydisperse assemblies and broad size distributions were obtained from the interaction of three different bacteriophage DNAs with PSS/DODAB biomimetic particles (149 and 309 nm mean diameter) over a range of [DNA] (Tables 4 and 5). Each DNA type (λ, T5, and T2-DNA) was added over the $1-10$ μg/mL range of DNA concentrations to two different bilayer-covered particulates and D_z or ζ were determined as a function of DNA concentration after interaction (1 h/25 °C). Figure 3 shows DNA concentration effect on ζ-average diameter (Figure 3A,C,E) and ζ-potentials of small cationic biomimetic particles (149 nm mean diameter) (Figure 3B,D,F). At 5, 7, and 8 μg/mL of λ, T5, and T2-DNA, respectively, ζ-potentials are close to zero and aggregation is extensive as depicted from maximal sizes. Above these concentrations, although redispersion occurs as evidenced by a certain decrease in mean particle sizes, large polydispersities still reveal a poor colloid stability over a range of DNA concentrations (Figure 3 and Table 4). Table 4 presents all mean diameters, ζ-potentials, and polydispersities for PSS137 particles, DODAB dispersion, and PSS/DODAB/λ, T5 or T2-DNA assemblies over a range of DNA concentrations. The lowest colloid stability and highest polydispersity were obtained for the DNA with the largest molecular weight over a range of negative ζ-potentials and DNA concentrations above charge neutralization.

Similar results were obtained for cationic biomimetic particles with 309 nm mean diameter (Figure 4). The λ, T5, and T2-DNA concentration effect on ζ-average diameter (Figure 4A,C,E) and ζ-potentials (Figure 4B,D,F) of the supramolecular assemblies yielded maximal size and zero of ζ-potential at 5, 6, and 6 μg/mL of λ, T5, and T2-DNA, respectively. Mean diameters, ζ-potentials, and polydispersity for PSS301 particles, DODAB dispersion and PSS/DODAB/λ, T5, and T2-DNA assemblies over a range of DNA concentrations are given in Table 5.

The comparison between polydispersity data for PSS137/DODAB (Table 4) and PSS301/DODAB (Table 5) reveals smaller values for the latter. This means that wrapping up DNA onto larger particles is easier than around smaller ones.

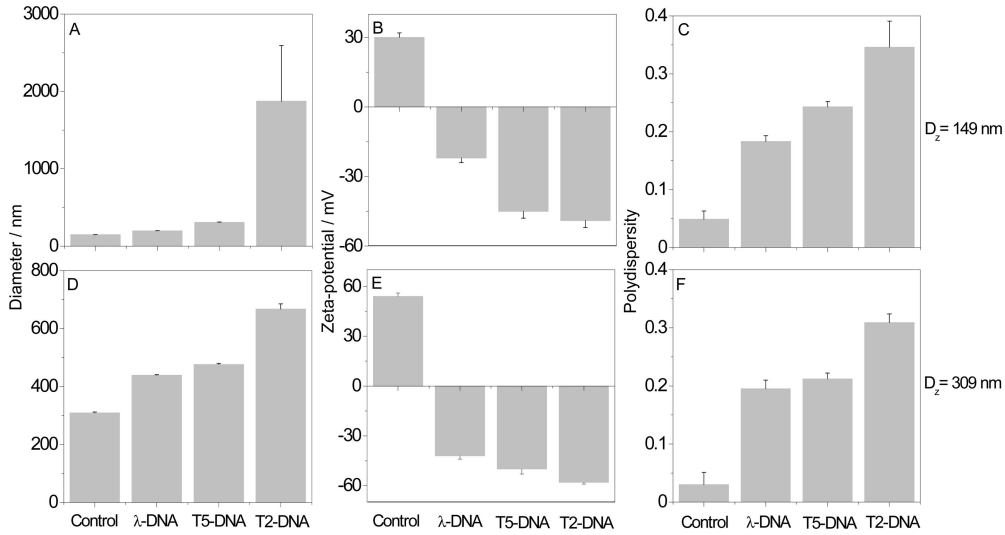

Figure 5. Effect of DNA type at 10 μg/mL [DNA] on mean particle diameter, ζ-potential, and polydispersity of PSS/DODAB/DNA assemblies for two different PSS/DODAB biomimetic particles built from PSS137 (A,B,C) and PSS301 (D,E,F).

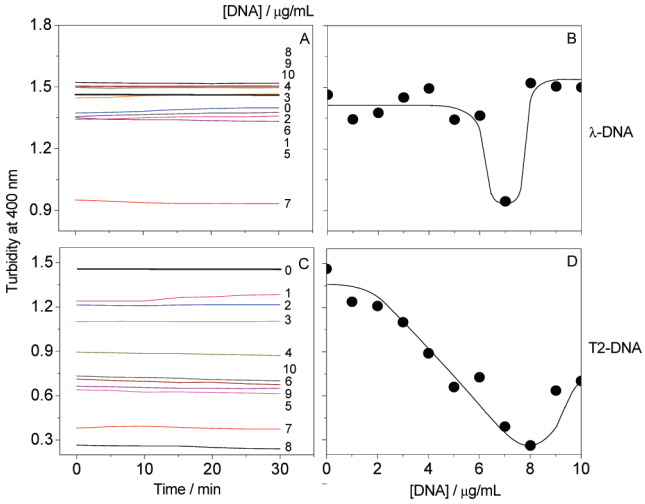

Figure 6. Effect of DNA type and concentration on turbidity kinetics (A,C) or turbidimetric titration (B,D) both at 400 nm for PSS301/DODAB/λ (A,B) and T2-DNA (C,D). Final concentrations of PSS and DODAB were 5×10^9 particles/mL and 0.02 mM, respectively.

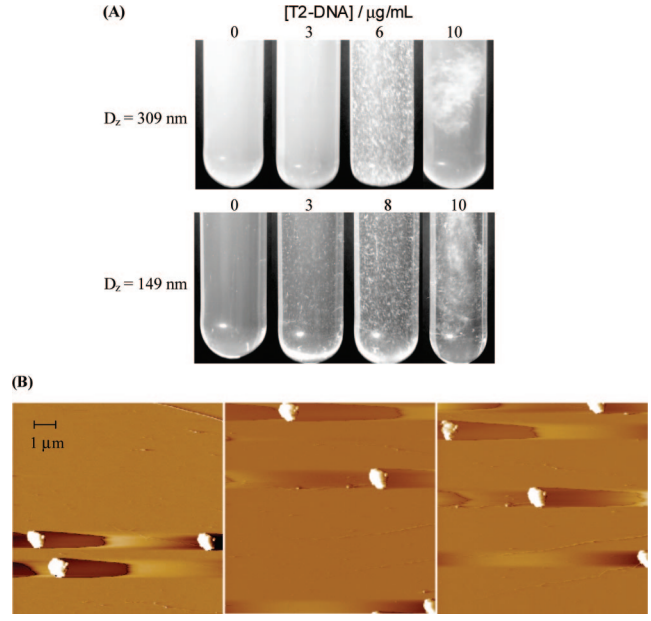

Figure 7. Macroscopic visualization of PSS/DODAB/T2-DNA dispersions in the test tubes over a range of T2-DNA concentrations (A). AFM topographic images of PSS137/DODAB/T2-DNA at charge neutralization (8 μg/mL DNA) (B).

In order to evaluate the effect of DNA type (λ, T5 and T2) on mean particle size, ζ-potential and polydispersity, DNA concentration was fixed at 10 μg/mL and the PSS/DODAB/DNA assemblies were built from two different PSS/DODAB biomimetic particles based on PSS137 (Figure 5A,B,C) or PSS301 (Figure 5D,E,F). DNA molecular weight increases in the order λ < T5 < T2 thereby increasing sizes, reducing ζ-potentials to produce more negatively charged particles and increasing substantially polydispersities of the supramolecular assemblies (Figure 5).

The effect of DNA length and concentration on turbidity kinetics of PSS301/DODAB/DNA assemblies was evaluated for two different DNAs (λ or T2-DNA) (Figure 6). Turbidity at 400 nm was recorded as a function of time after adding DNA to cationic biomimetic particles with 309 nm of mean diameter (Figure 6). The general behavior involved a very rapid attainement of a given turbidity upon DNA addition that remained constant over all observation time (30 min). When sedimentation could be visualized, low turbidity values at 400 nm were systematically obtained. Other general observation regards the range of DNA concentrations where low turbidity and extensive sedimentation is obtained; for both DNA types this occurred around 7 μg/mL (Figure 6). This is consistent with 6 μg/mL DNA as the DNA concentration required for zero ζ-potential and charge neutralization of the cationic biomimetic particle (Figure 4, Table 5). A major difference between λ and T2-DNA effects above 6−7 μg/mL DNA refers to the possibility of redispersion upon charge overcompensation. Only PSS/DODAB/λ-DNA assemblies are able to redisperse above charge neutralization (Figure 6B). PSS/DODAB/T2-DNA assemblies did not redisperse (Figure 6D). At 7 and 8 μg/mL of λ and T2-DNA, turbidity at 400 nm was 0.938 and 0.254 for PSS301/DODAB/λ, and PSS301/DODAB/T2-DNA assemblies, respectively. These values reveal sedimentation when compared to the control turbidity: 1.480 for PSS301/DODAB dispersion. In order to clarify microscopic organization of precipitated assemblies atomic force microscopy was performed.

Pictures of PSS/DODAB/T2-DNA dispersions and AFM topographic images are shown in Figure 7. Figure 7A shows PSS/DODAB/T2-DNA dispersions in test tubes as compared

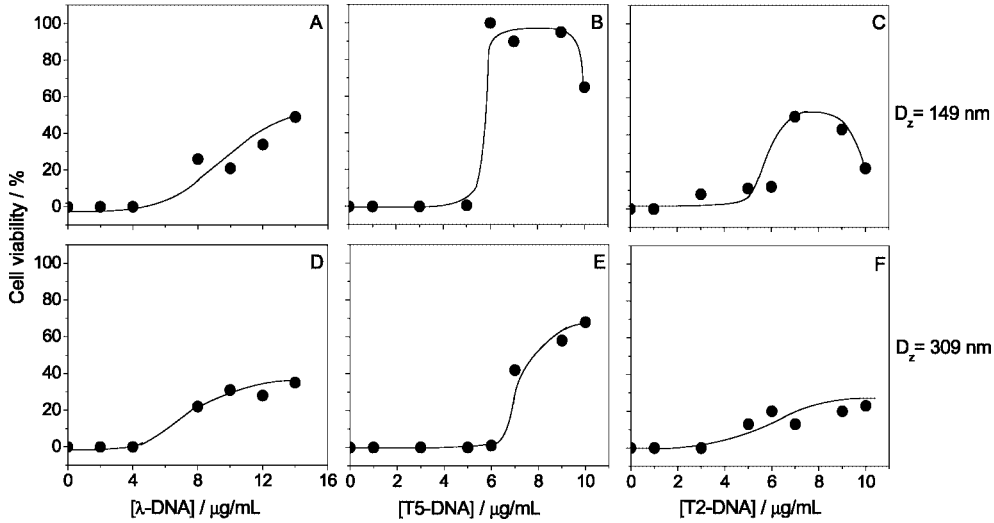

Figure 8. Effects of PSS/DODAB/DNA supramolecular assemblies on *E. coli* cell viability (%). Cationic biomimetic particles (149 and 309 nm) were covered with a final layer of λ-DNA (A,D), T5-DNA (B,E) and T2-DNA (C,F). Final concentrations of PSS137 and PSS301 are 2.4×10^{10} and 5×10^{9} particles/mL, respectively. Final [DODAB] is 0.02 mM. The final *E. coli* cells concentration for each sample is 1×10^{7} CFU/mL.

to controls without T2-DNA. Two sizes of cationic biomimetic particles were used: 309 and 149 nm. Similar photographs were obtained for the control without DNA and PSS/DODAB/T2-DNA dispersions at 3 μg/mL, an experimental condition where assemblies are still positively charged (Figures 3 and 4; Tables 4 and 5). However, at and above charge neutralization, flocculation and absence of redispersion above charge neutralization are evident (Figure 7A).

AFM images were obtained for PSS137/DODAB/T2-DNA at charge neutralization and 8 μg/mL of DNA (Figure 7B). Nucleosome-mimetic assemblies could be visualized where isolated, noninteracting particles were absent. All particles were attached to the long DNA chains and the most frequent image was the one of conglomerates very similar to those found in biological samples of wounded DNA around each nucleosome to form the conglomerates of solenoidal chromatin.[28] Artificial models of chromatin were recently developed from poly(L-lysine)-covered silica nanoparticles with 10, 15, and 40 nm mean diameter.[6] In this work, DNA was labeled with a fluorescent molecule so that giant bacteriophage DNAs compaction induced by cationic nanoparticles could be studied from fluorescence microscopy. However, much work devoted to the interaction between polyelectrolytes such as poly(L-lysine) and oppositely charged particles revealed that these assemblies display a low colloid stability.[29−32] In the present work, alternatively, we have employed cationic particulates with a narrow size distribution, low polydispersity, and high colloid stability. Therefore, aggregation and formation of supramolecular assemblies can only be ascribed to direct DNA effects.

Effect of PSS/DODAB/DNA Assemblies on *E. coli* Cell Viability. *E. coli* cell viability was affected by PSS/DODAB/DNA in diverse manner according to particle size, DNA type, and DNA concentration (Figure 8). These effects were evaluated for three bacteriophage DNAs previously submitted to interaction with two different cationic biomimetic particles of 149 and 309 nm. In Figure 8, cell viability is zero over a range of low DNA concentrations (0−5 μg/mL DNA) for which DNA negative charges were not enough to change the positive character of the cationic biomimetic particles. At and above charge neutralization, *E. coli* viability clearly improved. Assemblies including λ-DNA affected *E. coli* cell viability in similar ways for the two sizes of cationic biomimetic particles tested (Figure 8A,D). At and above charge neutralization for PSS/DODAB/DNA assemblies and for the same particle size, cell viability was higher for T5 and T2-DNA than for λ-DNA assemblies (Figure 8 panels B,E and C,F, respectively). A possible explanation for the lower cell viabilities in the presence of PSS/DODAB/λ-DNA is a better delivery of this shorter DNA chain by the cationic particles, since compaction of longer DNAs such as T5 and T2-DNAs would not be complete at the particle concentration employed in this study (see AFM image for T2-DNA in Figure 7B).

Regarding the effect of particle size on DNA delivery to *E. coli* cells, it was systematically observed that assemblies formed from smaller cationic biomimetic particles are less effective than the larger ones to decrease cell viability (Figure 8B,E and C,F). This might be associated with a lower capability for wounding DNA presented by the smaller particles so that long regions of the DNA strand will remain noncompacted and therefore, less "infective" regarding bacteria penetration of the phage DNA. In fact, these results agree with Zinchenko et al.[13] They found that DNA adsorbed amount per particle does increase with particle size.[13]

Cerritelli et al.[5] recently disclosed the magnificent assembly of encapsidated T7 DNA in the virus by means of cryo-electron microscopy. The degree of organization of this DNA in the bacteriophage assembled to capsid proteins though remarkable did not involve internal proteins. The whole assembly was 55 nm diameter.[5] While mimicking nature with cationic biomimetic particles, a question to be addressed is how a similar degree of compaction could be achieved by employing biomimetic systems and the limits of cationic nanoparticles for gene delivery. Usually, transfection experiments by cationic nanoparticles involve small plasmid DNAs with a few hundreds of base pairs.[9−11,33] However, the question of maximal length allowed for DNA delivery to bacteria by nanoparticles was not yet systematically studied and needs to be addressed. Other important issue regards the cytotoxicity of cationic compounds and nanoparticles against prokaryotic and eukaryotic cells in general.[34−36] In fact, the cationic PSS/DODAB/DNA assemblies containing only 20 μM DODAB over a range of low DNA concentrations (0−5 μg/mL DNA) resulted in 0% *E. coli* viability (Figure 8). Therefore, transfection performed by cationic nanoparticles may not be efficient since cells extensively

die in their presence. Perhaps, particles with slightly cationic, zero, or even negative charges will be more efficient for transfection due to lower cytotoxicity. We are presently evaluating transfection by the biomimetic particles over a range of sizes and charges.

Conclusions

Cationic biomimetic particles formed by PSS/DODAB are highly organized supramolecular and monodisperse particulates that can be obtained over a range of particle sizes (83−626 nm mean diameter of bare PSS particles) and be useful for physicochemical characterization of DNA assembly onto cationic particles. Cationic PSS/DODAB/bacteriophage DNA assemblies obtained over a range of particle sizes exhibit moderate colloid stability and polydispersity but high cytotoxicity against *E. coli*. Neutral PSS/DODAB/DNA assemblies extensively aggregate producing nucleosome mimetic systems that can be visualized by AFM. Anionic PSS/DODAB/DNA assemblies redisperse to a certain extent that is dependent on DNA length. For the longest DNA, redispersion is absent despite charge overcompensation. Over the low DNA concentration range, PSS/DODAB/DNA assemblies are cationic, colloidally stable with moderate polydispersity, and highly cytotoxic against *E. coli*. From DNA concentration corresponding to charge neutralization, neutral or anionic supramolecular assemblies PSS/DODAB/DNA exhibited low colloid stability, high polydispersity, and moderate cytotoxicity. Regarding particle size, assemblies obtained from smaller particles were more polydisperse than those resulting from the larger ones; apparently it is easier for DNA to be wrapped up around larger particles.

Acknowledgment. Financial support from FAPESP and CNPq is gratefully acknowledged. H.R. was the recipient of a MSc fellowship from CNPq.

References and Notes

(1) Li, W.; Suez, I.; Szoka, F. C. *Biochemistry* **2007**, *46*, 8579–8591.
(2) Luo, D.; Saltzman, W. M. *Nat. Biotechnol.* **2000**, *18*, 33–37.
(3) Gaweda, S.; Morán, M. C.; Pais, A. A. C. C.; Dias, R. S.; Schillén, K.; Lindman, B.; Miguel, M. G. *J. Colloid Interface Sci.* **2008**, *323*, 75–83.
(4) Kornberg, R. D.; Lorch, Y. *Cell* **1999**, *98*, 285–294.
(5) Cerritelli, M. E.; Cheng, N.; Rosenberg, A. H.; McPherson, C. E.; Booy, F. P.; Steven, A. C. *Cell* **1997**, *91*, 271–280.
(6) Zinchenko, A. A.; Luckel, F.; Yoshikawa, K. *Biophys. J.* **2007**, *92*, 1318–1325.
(7) Zinchenko, A. A.; Yoshikawa, K.; Baigl, D. *Phys. Rev. Lett.* **2005**, *95*, 2281011−228101/4.
(8) Lindsay, S. *Biophys. J.* **2007**, *92*, 1113.
(9) Kneuer, C.; Sameti, M.; Bakowsky, U.; Schiestel, T.; Schirra, H.; Schmidt, Lehr, H. C.-M. *Bioconjugate Chem.* **2000**, *11*, 926–932.
(10) Thomas, M.; Klibanov, A. M. *Proc. Natl. Acad. Sci. U.S.A.* **2003**, *100*, 9138–9143.
(11) Roy, I.; Ohulchanskyy, T. Y.; Bharali, D. J.; Pudavar, H. E.; Mistretta, R. A.; Kaur, N.; Prasad, P. N. *Proc. Natl. Acad. Sci. U.S.A.* **2005**, *102*, 279–284.
(12) Golovlev, V. V.; Sun, Y.; McCann, M. P.; Fan, W.-H. *U.S. Pat. Appl. Publ.* **2008**, 48.
(13) Zinchenko, A. A.; Sakaue, T.; Araki, S.; Yoshikawa, K.; Baigl, D. *J. Phys. Chem. B* **2007**, *111*, 3019–3031.
(14) Rejman, J.; Oberle, V.; Zuhorn, I. S.; Hoekstra, D. *Biochem. J.* **2004**, *377*, 159–169.
(15) Hoekstra, D.; Rejman, J.; Wasungu, L.; Shi, F.; Zuhorn, I. *Biochem. Soc. Trans.* **2007**, *35*, 68–71.
(16) Carmona-Ribeiro, A. M.; Midmore, B. R. *Langmuir.* **1992**, *8*, 801–806.
(17) Tsuruta, L. R.; Lessa, M. M.; Carmona-Ribeiro, A. M. *J. Colloid Interface Sci.* **1995**, *175*, 470–475.
(18) Lessa, M. M.; Carmona-Ribeiro, A. M. *Colloids Surf., A.* **1999**, *153*, 355–361.
(19) Pereira, E. M. A.; Vieira, D. B.; Carmona-Ribeiro, A. M. *J. Phys. Chem. B* **2004**, *108*, 11490–11495.
(20) Petri, D. F. S.; Carmona-Ribeiro, A. M. Biomimetic Particles. In *Polymeric Nanostructures and Their Applications*; Nalwa, H. S., Ed.; American Scientific Publishers: Stevenson Ranch, CA, 2007; Vol. 1, pp 485−530.
(21) Lincopan, N.; Rosa, H.; Carmona-Ribeiro, A. M. *Macromol. Symp.* **2006**, *245*, 485–490.
(22) Carmona-Ribeiro, A. M. *Chem. Soc. Rev.* **1992**, *21*, 209–214.
(23) Schales, O.; Schales, S. S. A. *J. Biol. Chem.* **1941**, *140*, 879–884.
(24) Lincopan, N.; Espíndola, N. M.; Vaz, A. J.; Carmona-Ribeiro, A. M. *Int. J. Pharm.* **2007**, *340*, 216–222.
(25) Carmona-Ribeiro, A. M. *Chem. Soc. Rev.* **2001**, *30*, 241–247.
(26) Grabowski, E.; Morrison, I. *Measurements of Suspended Particles by Quasi-Elastic Light Scattering*; Wiley-Interscience: New York, 1983; p 199.
(27) Claesson, P.; Carmona-Ribeiro, A. M.; Kurihara, K. *J. Phys. Chem.* **1989**, *93*, 917–922.
(28) Stryer, L. *Biochemistry*; W. H. Freeman and Company: New York, 1981; Chapter 29.
(29) Reis, E. A. O.; Caraschi, J. C.; Carmona-Ribeiro, A. M.; Petri, D. F. S. *J. Phys. Chem. B.* **2003**, *107*, 7993–7997.
(30) Vieira, D. B.; Lincopan, N.; Mamizuka, E. M.; Petri, D. F. S.; Carmona-Ribeiro, A. M. *Langmuir* **2003**, *19*, 924–932.
(31) Correia, F. M.; Petri, D. F. S.; Carmona-Ribeiro, A. M. *Langmuir.* **2004**, *20*, 9535–9540.
(32) Zuzzi, S.; Cametti, C.; Onori, G. *Langmuir.* **2008**, *24*, 6044–6049.
(33) Li, Z.; Li., Z.; Zhu, S.; Gan, K.; Zhang, Q.; Zeng, Z.; Zhou, Y.; Liu, H.; Xiong, W.; Li, X.; Li, G. *J. Nanosci. Nanotechnol.* **2005**, *5*, 1199–1203.
(34) Carmona-Ribeiro, A. M. *Curr. Med. Chem.* **2003**, *10*, 2415–2446.
(35) Carmona-Ribeiro, A. M.; Ortis, F.; Schumacher, R. I.; Armelin, M. C. S. *Langmuir* **1997**, *13*, 2215–2218.
(36) Pereira, E. M. A.; Kosaka, P. M.; Rosa, H.; Vieira, D. B.; Kawano, Y.; Petri, D. F. S.; Carmona-Ribeiro, A. M. *J. Phys. Chem. B* **2008**, *112*, 9301–9310.

JP806992F